A REPORT

ON

OBSERVATIONS OF 6.67GHz RADIO RECOMBINATION LINES WITH 10.4m TELESCOPE

By

Ramanpreet Kaur

M.Sc. (HS) Physics

Guru Nanak Dev University

Amritsar, Punjab

Under the guidance of **Prof. N. Udayashankar**

Summer School project

Raman Research Institute

2002

TABLE OF CONTENTS

Chapter 1
Introduction

1.1 Astronomy

Astronomy is the scientific study of matter in the outer space, especially positions, dimensions, distance, motion, composition, energy and about evolution of celestial bodies and phenomenon. From the dawn of civilization, astronomy has provided important stepping stones for human progress. Our calendar and system of timekeeping came from astronomy. Much of today's mathematics is the result of astronomical research. Trigonometry was invented by Hipparchus, a Greek astronomer. The calculus, the basis of all modern science and engineering, was invented by Sir Issac Newton for astronomical calculations. Astronomy provided the navigational techniques that allowed sailors and aviators to explore our planet (and today allow spacecrafts to explore our solar system). Astronomy's appetite for computational power drove the development of many of the earliest electronic computers. The space age, which brought us the communication and weather satellites upon which we depend each day, would have been impossible without the fundamental knowledge of gravity and orbits discovered by astronomers. At today's observatories, the needs of astronomers for better instruments continue to drive developments in such diverse fields as electronics, mechanical engineering, and computer science.

Astronomy offers scientists from a wide range of backgrounds with a nearly infinite variety of cosmic "laboratories" for observing physical phenomena. It is unlikely that any laboratory on Earth will ever produce matter as dense as that of a neutron star, temperatures as hot as those inside a supernova, or gravity as strong as that of a black hole. Yet, astronomers can study the physics of such extreme

conditions routinely with instruments such as the Giant Meterwave Radio Telescope (GMRT). The technique of Very Long Baseline Interferometry (VLBI) is a primary tool providing valuable data on the drift of Earth's continents and the mechanisms of global climate.

I find astronomy as an exciting, visual science easily accessible to amateur observers. Astronomy stirs scientific curiosity in thousands of young people, because it involves nearly the whole range of the physical sciences, including mathematics, physics, chemistry, geology, engineering and computer science.

Astronomy, by providing the excitement of new knowledge about the fascinating variety of strange objects in the universe, can help communicate much basic science to all our people.

1.2 Radio Astronomy: An overview

Radio astronomy is the study of distant objects in the universe by collecting and analyzing the radio waves emitted by those objects. Radio astronomers can make images using the radio waves emitted by such objects, as well as by gas, dust and very energetic particles in the space between the stars. Radio astronomy has been a major factor in revolutionizing our concepts of the universe and how it works. Radio observations have provided a whole new outlook on objects we already knew, such as galaxies, while revealing exciting objects such as pulsars and quasars that had been completely unexpected. From revealing the remnant of the Big Bang to showing the afterglows of the superenergetic Gamma Ray Bursts, radio observers have provided science with insights unobtainable with other types of telescopes. Of the ten astronomers who have won the Nobel Prize in Physics, six of them used radio telescopes for the work that won them the Nobel. Radio telescopes today are among the most powerful tools available for astronomers

studying nearly every type of object known in the universe.

Since its beginning, less than 70 years ago, radio astronomy has done much to transform our understanding of the universe. Our eyes see only a small part of the electromagnetic spectrum. If we could see the universe through radio sensitive eyes, it would appear quite different. The Sun would often burst into brilliant displays of transforming "colors". Jupiter, on occasion, would explode into a stormy stream of pulses and sparkles. The Milky way would be visible in the daytime and the brightest "stars" would not be stars at all, but distant galaxies and torrential supernovas.

1.3 Optical and Radio Astronomy: A comparison

Origins of astronomy dates back to prehistoric times. However, until as recent as 1932, the exploration of the universe was carried out only with the help of optical telescope. Only the light emitted in the visible band of the electromagnetic spectrum was used for astronomical investigations.

Radio astronomy, which originated with Jansky's detection of radio emission from the Galactic center (in 1932) was the first non-optical branch of Astronomy. The positions of radio and optical astronomy in the electromagnetic spectrum coincide with the two principle transparent bands of the earth's atmosphere and ionosphere. Those transparent bands are commonly referred to as the optical and radio windows. A graph showing the relative transparency of the earth's atmosphere is shown below, with the transparency as ordinate ranging from 0 (opaque) to 1 (perfectly trasparent) as a function of wavelength on a logarithmic scale.

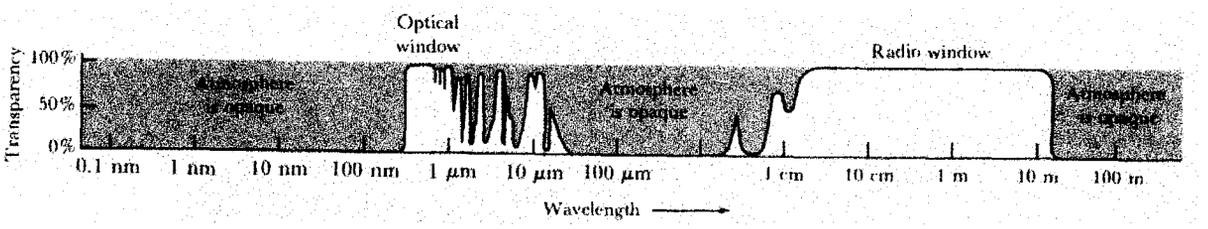

The optical window extends from about 0.4 to 0.8 micron while the much broader radio window extends from about 1cm to 10m. The wavelength limit is a function of the atmospheric composition, cloud cover, etc, while the long wavelength limit depends on the electron density in the ionosphere. This, in turn, is a function of the time of the day, solar activity etc.

1.4 The history of Radio Astronomy

The history of radio astronomy begins in 1931 when an American engineer named Karl Jansky, while working for Bell Telephone Laboratories, conducted experiments on radio wavelength. Jansky detected three separate groups of static; local thunderstorms, distant thunderstorms and a steady hiss-type static of unknown origin. The unknown source that Jansky found is the center of the Milky Way as he was able to show by determining its position on the sky. Jansky was the first to detect radio emission from the Galaxy. The image below shows Jansky standing with his rotation allowed it to move along with the static. The work done by Jansky included receiving frequencies in the range of 15 to 30 MHz ($\lambda \sim 15$m).

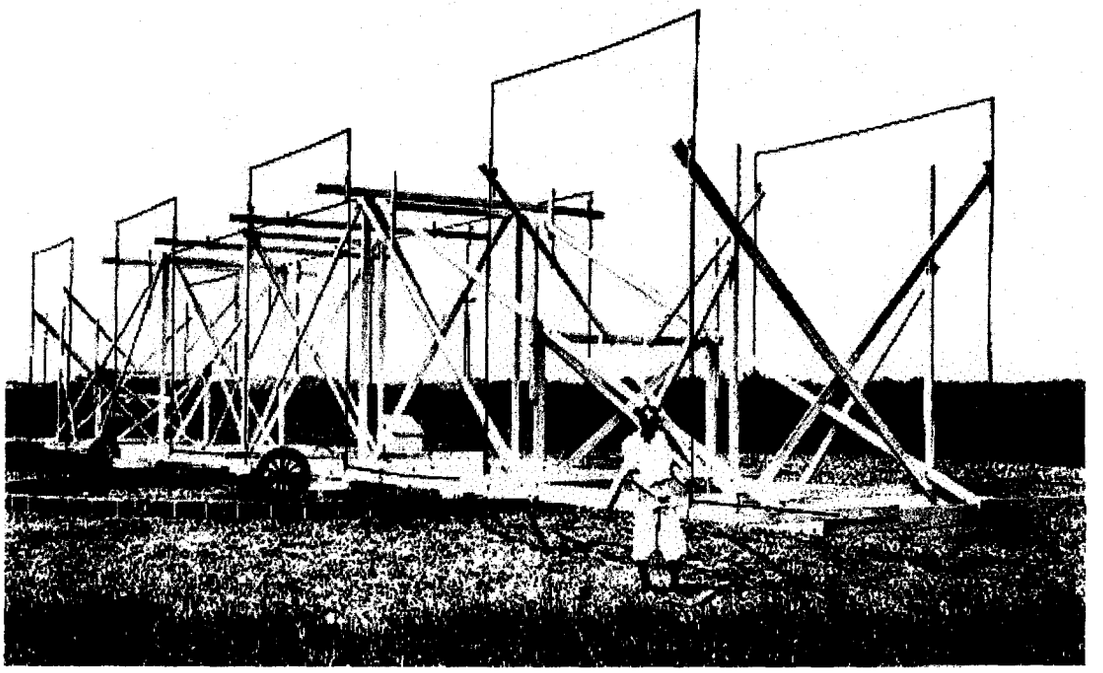

In 1937 Grote Reber, also a radio engineer, built a parabolic, 9.5-m diameter, reflector dish in his backyard. This was the first radio telescope used for astronomical research.

The first observation of radio emission from the sun was made in 1942, by J.S. Hey. In 1946, J.S. Hey, S.J. Parsons, and J.W. Phillips observed fluctuations in the intensity of cosmic radio waves from the constellation Cygnus. In the next ten years thousands of discrete sources were identified, including galaxies and supernovae.

In 1951, H. I. Ewen and E. M. Purcell, detected the spectral line emission from neutral Hydrogen that fell into the radio spectrum. For the first time, astronomers could determine the shape of our own home galaxy. This major discovery made by Penzias and Wilson was the cosmic background radiation and the strongest evidence for the big bang. Penzias and Wilson won the Nobel Prize in physics for their discovery in 1978.

In the late 1960's, radio pulsars, predicted only by theories of stellar evolution, were discovered by Jocelyn Bell-Burnell and Anthony Hewish. Bell-Burnell and Hewish were working at what is now called the Nuffield Radio Astronomy Observatory at Cambridge, England. Pulsars are very strongly magnetized, spinning neutron stars. Anthony Hewish and Martin Ryle won the Nobel prize for this discovery in 1974.

Chapter 2

Co-ordinate systems used in Astronomy

To an observer on the earth there are several coordinate systems, which are useful in dealing with positions of celestial objects.

2.1 Horizon system:

In this system, a plane through the observing point parallel to the horizon is the plane of reference. In the figure, the poles are the zenith (point overhead) and nadir (point underfoot). The vertical circle through a celestial object and the zenith is the object circle. The co-ordinates of the object are then given by the azimuth, or horizontal angle measured from an arbitrary reference direction (usually north) clockwise to the object circle, and the altitude, or elevation angle measured upward from the horizon to the object. The great circle through the north and the south points and the zenith is the meridian.

2.2 Equatorial co-ordinates:

In this system the earth's equator is the plane of reference. The poles are at the intersection of the earth's axis with the celestial sphere, an imaginary surface at a large distance with the earth at its center. The poles are the north celestial pole (NCP) and the south celestial pole (SCP). The circle at the intersection of the plane of the earth's equator and the celestial sphere is the celestial equator. The great circle throught the celestial poles and the object is the object's hour circle, and the great circle which passes through the celestial poles and the zenith is the meridian circle. The co-ordinates of the celestial object are given by the declination, or angle between the celestial equator and the object, and the right

ascension, or angle measured from an arbitrary reference direction (the vernal equinox) to the object's hour circle. The declination is expressed in degrees and is positive if the object is north of the equator and negative if south ($-90^{o} \leq \delta \leq +90^{o}$). Right ascension is measured eastward from the vernal equinox and is expressed either in degrees ($0^{o} \leq \alpha \leq 360^{o}$) or, more commonly, in hours, minutes and seconds of time ($0^{h} \leq \alpha \leq 24^{h}$).

The right ascension and declination of a celestial object define its position in the sky in a relatively fixed manner, which is independent of the earth's diurnal rotation. However, because of the gradual precession of the earth's axis around the pole of the ecliptic, there is a slow change in the equatorial co-ordinate for any fixed object in the sky. This change makes one cycle in about 26,000 years. Hence, to be explicit it is necessary to specify the date to which the right ascension and the declination refer. This date is called the epoch, say for eg. epoch 2000.0 corresponds to the right ascension and declination on the date of January 1st, 2000.

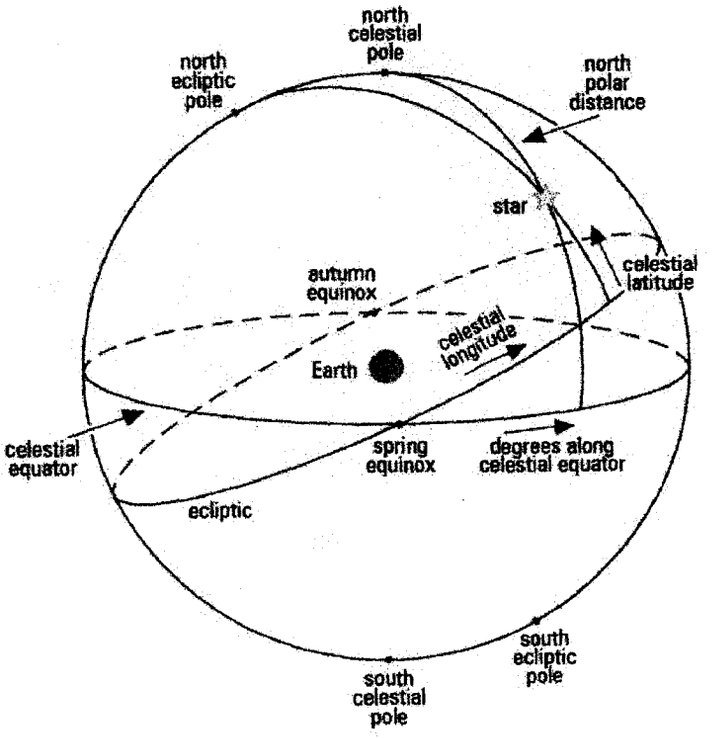

2.3 Ecliptic system of co-ordinates:

In this system, the ecliptic, or the plane through the earth's orbit is taken as the reference. The orbits of most of the planets lie close to this plane (within 7^{o} except for Pluto). The co-ordinates are the celestial longitude, measured eastward along the ecliptic from the vernal equinox, and the celestial latitude, measured north (+) or south (–) from the ecliptic. This system is useful mainly in the studies of the solar system.

2.4 Galactic co-ordinates:

In this co-ordinate system, a plane through the earth parallel to the plane of the Galaxy is taken as the plane of reference. The reference point is the direction towards the center of the Galaxy. The Galactic longitude, l and latitude, b are both measured in degrees. Galactic latitude is measured in the range $-90^{o} \leq b \leq +90^{o}$ (from the south Galactic pole to the North Galactic pole) and the longitude increases from 0^{o} to 360^{o}.

Chapter 3

The Interstellar medium: An overview

The space between the stars in the Galaxy is filled with the gas containing hydrogen, helium, carbon, calcium and many other elements and dust grains. This constitute the interstellar medium (ISM). The ISM is observed to be highly inhomogeneous with most of the mass being concentrated in clouds, both atomic and molecular, which occupy a small fraction of the volume in the Galaxy. The rest of the volume is filled by a warmer all pervading intercloud gas. Matter in some parts of the ISM condense to form stars. In other parts, stars explode as supernovae, thus returning matter back to the ISM, and enriching it in heavier elements which are synthesized inside the stars. Thus the ISM is a dynamic system in our Galaxy, in which there is a constant exchange of matter and energy between its different components and also between it and the stars. The energetics of the ISM are governed mainly by the mass exchange between the massive stars and the ISM.

Hydrogen is the most abundant species in the Galaxy – both in the ISM and in stars. Helium comes next with a cosmic abundance of 0.1 by number, if the abundance of hydrogen is 1. The abundance of all other elements are much less (~ 10^4 and below).

3.1 The different phases in the ISM:

3.1.1 Ionized clouds (HII regions):

All the hydrogen in the vicinity of the hot O & B stars where the Ultraviolet (UV) flux (with $\lambda > 912$ Å; $hc/\lambda > 13.6$ eV, the ionization potential of hydrogen

atom) is intense, exists in the ionized form known as HII regions. Helium, which has the first ionization potential = 24.4 eV is also expected to be singly ionized close to the O & B stars. While the electrons that are freed in the ionization process provide the heating in this region, collisionally-excited, forbidden lines of oxygen and other heavier elements act as the cooling agent. These cooling and heating processes establish equilibrium temperatures in these regions in the range (5 to 10) $\times$ 10^3 K, whereas the electron densities range from 10 to 10^4 cm^{-3}. Recombination of electrons with ions is the intense process which balances the process of ionization. If the electron recombines to an excited state, then recombination lines are emitted as the electron cascades down to the ground state. The Balmer Hα, Hβ and higher frequency (υ > 1 GHz) radio recombination lines of hydrogen are readily observed from HII regions. These ionized regions are not in pressure equilibrium with the ISM, because of high pressure these regions expand into the surrounding medium.

3.1.2 Atomic phase:

More than 95% of the mass in the ISM is in the form of neutral hydrogen (almost equal mass in the atomic & molecular forms) and helium. Atomic hydrogen (HI) is thus an important phase of the ISM. The HI gas is all pervasive and its radial distribution in the Galaxy is distinct from that of ionized and molecular gas. Regions of atomic hydrogen have temperatures ranging from 30 – 8000 K and a wide range of densities. These different components are in pressure equilibrium with typical pressures, P/k (where P = nkT, is the gas equation) of ~ 4000 cm^{-3} K. HI gas exists in the form of discrete clouds as well as a diffuse component pervading the entire Galaxy.

3.1.3 Molecular phase:

Molecular clouds are the densest regions of the ISM and the star formation

activity is associated with them. Much of the molecular gas appears in the form of Giant Molecular Clouds (GMC) which are self-gravitating. The pressure in these clouds is much larger than the thermal pressure observed in the diffuse ISM. The gas surface density of molecular hydrogen exceeds that of atomic and ionized hydrogen in the central regions of the Galaxy. Typical temperatures in the molecular clouds is 10 – 20K, which is the expected equilibrium temperature for a balance between heating by low energy cosmic rays and cooling by the rotational transitions in Carbon Monoxide. Hydrogen densities in molecular clouds range from $10^3 - 10^6$ cm^{-3}.

3.2 Radio Spectral Lines

Above three types of objects correspond to, in a sense, three evolutionary stages of ISM. These objects exhibit distinct spectral signatures in the radio frequency range. Therefore, radio spectral lines are classified as:

3.2.1 The 21cm neutral Hydrogen line

This line arises in the ubiquitous neutral atomic hydrogen which occurs in the form of cold clouds and also as a hot intercloud medium, and was first predicted by Van de Hulst(1945). This line was subsequently detected by two groups almost simultaneously (Ewen and Purcell 1951 and Muller and Oort 1951). This line arise from the magnetic hyperfine transistion in the ground state of atomic hydrogen.

3.2.2 Centimeter and millimeter wavelength molecular lines

The posssibility of detecting molecular lines from interstellar space was first predicted by Shklovsky (1949). Most of these lines are observed from giant molecular clouds. These clouds or cloud complexes are believed to be sites of star formation. These spectral lines arises due to transitions between the doublet

ground state rotational levels of OH and CO. Some of the lines from molecules like OH, H_2O, SiO etc are intense and they arise from exotic phenomena like masers.

3.2.3 Radio Recombination lines

Kardashev (1959) first predicted the possibility of observing radio recombination lines of hydrogen and helium in the radio frequency range, from ionized regions in the intersteller space. The prediction was subsequently confirmed by Dravskikh and Dravskikh (1964) who detected the recombination line arising due to the transition from n = 105 to n = 104 in the direction of M17 and orion nebula. The recombination lines arise in clouds which are more or less completely ionized (HII regions) by young hot stars which are embedded in them.

Chapter 4

Radio Recombination Lines: A Review

Kardeshev (1959) predicted that radio recombination lines of hydrogen and helium would be observable from ionized gas in the galaxy. The observation and interpretation of radio recombination lines has become an important branch of radio astronomy. These lines have been observed over the entire radio frequency window. Recombination lines are formed when an excited electron in an atom makes transitions between different energy levels. These lines cover a wide range of frequencies, appearing in UV (Lyα, n = 2 $\rightarrow$ 1) to long radio wavelengths (~ 15m, n ~ 730). Kardeshev's prediction was confirmed when Dravskikh & Dravskikh (1964) and Sorochenko & Borozich (1964) reported the first detection of the hydrogen Radio recombination line (RRL) at ~ 5.2cm (H104 at 5.763 GHz) from the Omega nebula. Since then, RRLs of hydrogen, helium and carbon have been detected from a variety of regions. Obsrvations of RRLs are useful for several reasons as listed below:

- To determine various physical properties such as temperature, density, and turbulence of different types of ionized gas.
- To investigate distant optically obscured HII regions.
- To determine the large scale structure of the Galaxy as traced by the ionized gas.
- To obtain the helium abundance.
- To distinguish between thermal and non-thermal sources (e.g. HII regions and supernova remnants).

4.1 Physical processes in HII regions

HII regions are gaseous clouds in the interstellar medium which are more or less completely ionized by the ultra violet radiations from one or more hot stars having surface temperatures in excess of 30,000 K. Most of the radio recombination lines arise from such regions and because of the finite flux of the ultra violet photons emitted by the hot stars, they can only ionize a finite volume of the gas. Therefore if the star is a sufficiently large cloud, then the ionization can occur only up to a certain distance, outside of which the gas will be neutral. This is usually a sharp transition between ionized and neutral regions. The boundary of ionization will be rather symmetric about the exciting star and the ionized region, is also known as the "strÖmgren sphere". In a steady state, the number of ionizations is balanced by the corresponding number of recombinations and an ionization equilibrium is established. The photo-electrons liberated during the ionization carry the excess energy of the ionizing photons as their kinetic energy. The free electrons immediately establish a Maxwellian velocity distribution through collisions among themselves and with the ions. The cross-section for elastic collisions among electrons exceed by a large factor all other nebular cross sections including recombination. Maxwellian distribution of velocity among the particles is established. The difference in energy of an electron when it was created during the photo-ionization and its energy when it undergoes recombination goes into heating of the nebular gas. This is the main source for heating of the ionized region. In thermal equilibrium, this heating is balanced by cooling mechanisms, in which the electron looses energy through inelastic collisions with protons and particularly the heavy ions present in the nebula. The main source of cooling is the electron collisional excitation of the lying bound levels of reasonably abundant elements such as oxygen, nitrogen and sulphur, followed by spontaneous emission of photons which escape from the nebula.

Electrons also loose some amount of energy during their other encounters with ions, which result in free-free emission that is thermal bremsstrahlung. The temperature of the nebular gas is determined by the balance between heating by photo-ionization and cooling, largely by collisional excitation of the bound levels of trace elements followed by emission of photons. The resulting temperatures are generally in the range 6,000 – 10,000 K. The factors which determine the temperature of the nebula are the abundance of trace elements like O, N, Ne, S, etc., the electron density N_e and to a lesser extent the effective temperature of the exciting star. If N_e is increased, temperature of the nebula will increase, since the excited levels of the trace elements become de-populated by collisional de-excitation and not by radiative transition which serve to cool the nebula. An increase in the abundance of trace elements will decrease the nebular temperature as the above cooling process becomes more effective. However high effective temperature of the exciting stars usually results in a higher ionization of the trace elements and not in a higher nebular temperature.

4.2 Nomenclature for the RRLs

The recombination lines are designated as Xnα, Xnβ etc. where X is the chemical symbol of the emitter (H, He, C, etc.) and n is the quantum number of the lower level. α, β etc. represent changes in Δn of 1, 2, etc. due to the transition.

4.3 Recombination line profile

A recombination line (RL) is emitted by an atom when a bound electron jumps between two quantum levels; the energy difference between the two levels appearing as a spectral line. The energy of the spectral line is not confined to a single frequency but spread over a range of frequencies determined by many broadening mechanisms. In addition to natural broadening, which arises due to the finite life time of the quantum level, other mechanisms, described below, act to

broaden the line further. Depending on the dominant broadening mechanisms, there can be two different shapes for the observed line profile.

4.3.1 Gaussian profile

Velocities of the particles in thermal equilibrium follow the maxwellian distribution. The distribution of velocity of the particles emitting at a certain frequency results in a distribution of frequencies when seen in the observer's frame due to the doppler effect. The resulting spectral distribution is a Gaussian. The width of the spectral line given by

$$\Delta V_D = 2\sqrt{\ln 2}\left[\frac{2kT_D}{M_i}\right]^{1/2}$$

where

T_D is the doppler temperature

Mi is the mass of the emitting atom

k is the Boltzmann's constant 1.38×10^{-23} Joule K^{-1}

The Doppler temperature includes contributions from both thermal and turbulent motions in the plasma. In most of the spectral lines arising in the ISM, the line width is dominated by turbulence. Hence only an upper limit on the kinetic temperature for the plasma can be derived from the thermal line width. With increasing plasma temperatures and turbulance, the Doppler width increases and the peak line intensity decreases, keeping the integrated line strength constant.

4.3.2 Lorentzian profile

Natural, pressure and radiation broadening results in a Lorentzian–shaped profile for the RRL. Natural broadening is a result of the finite lifetime of the energy level. Pressure broadening is sensitive to the electron density in the cloud.

Under the conditions prevailing in the ISM, electron impacts with the emitting atom is the major contributor to pressure broadening. If an atom undergoes a collision with an electron in the plasma while it is emitting a spectral line, the phase of the emitted wave will be suddenly modified. In a sea of colliding and radiating atoms, this process leads to broadening of the emitted line and the resulting profile shape is a lorentzian. This function has the form

$$\phi_L = \frac{\gamma}{\pi} \frac{1}{\left[(\nu' - \nu)^2 + \gamma^2\right]}$$

An external radiation field incident on a plasma can enhance the downward transition out of an atomic level by stimulated emission. This is called the radiation broadening and it can increase or even dominate the decay rate of a level. Through this process, the lifetime of a level is reduced, the line width is increased and the resulting profile is a lorentzian. Pressure and radiation broadening are strong functions of the principal quantum number.

4.4 Radio continuum emission

Radio continuum radiation from an ionized gas arises from thermal bremsstrahlung, also called free free radiation, during encounters of the free electrons in the gas with positive ions.

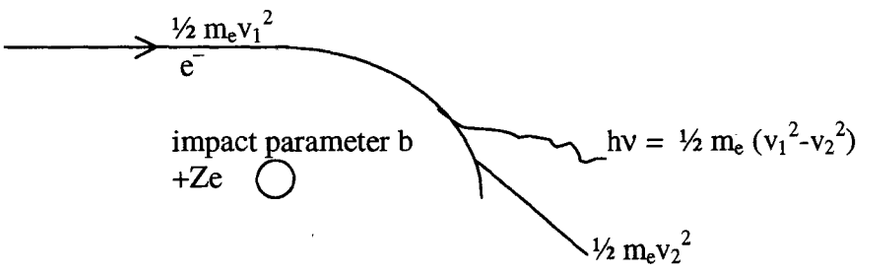

Radio Continuum Emission.

An electron of initial kinetic energy ½ mv_1^2, on coulomb interaction with a charge +Ze gets deflected and radiates and goes out with a reduced final energy ½mv_2^2. The difference between the initial and final energies is emitted as a photon, which can escape from the nebula. A summation of the energies lost by the electrons in several such encounters with different impact parameters b and different initial and final energies accounts for the continuum radiation from the nebula, most of which appears at radio frequencies. The radio continuum radiation, although it contributes very little to the energetics of an HII region, provides a very powerful tool for studying such objects at large distances in the galaxy, since at these frequencies interstellar extinction is practically absent.

4.5 Recombination line frequencies

The frequency υ, of a transition from an upper level of principal quantum number m to a lower level n is given by the Rydberg formula

$$\upsilon = R_a c Z^2 (1/n^2 - 1/m^2)$$

Where υ = the rest frequency of the emitted photon

m = principal quantum number at which the transition begins

n = principal quantum number at which the transition ends

c = the velocity of light = 2.99272×10^8 m s^{-1}

Z = effective nuclear charge of the recombining ion

R_a = $1097.3731\ (1 + m_e/M_a)m^{-1}$ is the Rydberg constant for an element a

M_a = atomic mass

m_e = electronic mass = 9.11×10^{-31} Kg

For most practical purposes where $\Delta n = (m - n) << n$ (radio frequencies) the above equation can be approximated by

$$\upsilon = 2R_a c Z^2 \Delta n / n^3$$

4.6 Electron temperature of the HII region

If RRLs are emitted under conditions close to local thermodynamic equillibrium (LTE) then the ratio of the line strength to the thermal radio continuum from the ionized gas can be directly related to the electron temperature of the nebula. This can happen at frequencies where the nebula is optically thin. Then in the absence of a background radiation field, the LTE ratio of the line to continuum brightness temperatures is the ratio of the optical depths.

$$T_l/T_c = \tau_l/\tau_c$$

The LTE electron temperature is given by (Roelfsema & Goss, 1992)

$$T_e^* = \left[6943 \nu^{1.1} \frac{1}{(T_l/T_c)} \frac{1}{\Delta V_D} \frac{1}{\left(1+Y^+\right)} \right]^{0.87} \text{K}$$

Once we know the electron temperature, we can use this value in the equation for doppler broadening to estimate the thermal velocity width of the spectral line.

$$\Delta V_{th} = 2[2kT_e \ln 2 / M]^{1/2}$$

where , k is the Boltzmann's constant and M is the mass of the ion

The velocity of turbulence can obtained from the relation

$$\Delta V_{obs}^{2} = \Delta V_{th}^{2} + \Delta V_{tur}^{2}$$

Chapter 5

Observations and Results

In the study of the radio recombination lines from the HII regions, we concentrated our attention to the study of H99α lines. The value of the frequency of radiation of H99α line is 6.67797 GHz. The observations were carried out using the 10.4-m radio telescope, at RRI in Bangalore.

In our experiment, we observed 8 sources and we were able to detect the spectral lines from six sources. The sources and their co-ordinates are given in the following Table:

Source Names	J2000 R.A. (h m s)	J2000 Dec. (^{0} ' ")	Gal. Longitude (deg)	Gal. Latitude (deg)
M42	05 35 11.9	–05 23 16	209.01	–19.38
M16	18 18 51.9	–13 45 46	16.95	0.79
NGC6334	17 20 37.2	–35 45 59	351.15	0.47
NGC6357	17 25 19.3	–34 21 52	353.17	0.89
NGC2736	08 59 07.9	–47 35 01	266.90	0.12
M17	18 23 52.2	–16 09 19	15.10	–0.75
M19	17 02 36.00	–26 16 00	356.87	9.38
M20	18 02 18.00	–23 02 00	7.09	–0.29

5.1 Calculation of system temperature (T_{sys})

There is no direct method to calculate the system temperature. We first observed the voltage V_{hot} that is proportional to the temperature of the system and surroundings. For this we moved the radio telescope such that the antenna is pointing to the surroundings i.e.; at ~0° elevation (fap). Thus,

$$V_{hot} \alpha T_{hot} + T_{sys}$$

Then we lifted the antenna to 45° elevation using manual mode. Then there is only T_{sys} and the corresponding voltage V_{sky} can be noted from the computer.

$$V_{sky} \alpha T_{sys}$$

Using the two equations given above, we can calculate the T_{sys} as

$$T_{sys} = T_{hot} / [(V_{hot}/V_{sys}) - 1]$$

We assume T_{hot} as 250 K

Date	V_{hot} (volt)	V_{sys} (volt)	T_{sys} (K)
12-6-2002	1.6403	0.4925	107.30
14-6-2002	1.6638	0.4966	106.30
15-6-2002	1.6411	0.4796	103.20
15-6-2002	1.6391	0.4896	106.50
17-6-2002	1.5757	0.4742	107.60
18-6-2002	1.4692	0.4460	108.97

There are four computers to control the working of the telescope and to get results. First computer is known as the control p.c. (c.p.c), which controls the motion of the telescope. The second one is the health monitoring p.c. (h.m.p.c) that monitors the health of the each component of the telescope. The third one is the high-resolution spectrometer p.c. (h.r.s.p.c) which produces the autocorrelation power as a function of frequency. The last p.c. is used to do the necessary calculations and to get the result of the observations.

5.2 Spectral Line Observations

For the line observations, we used a bandwidth of 5.92 MHz and 4096 channels. Each source was observed for an hour each. In the event of a non detection, the observing time was extended by one more hour. The data reduction was carried out using the UNIPOPS package from the National Radio Asrtronomy Observatory (NRAO). The final spectra were fitted with Gaussians using the same package.

5.3 The Continuum Observations

In continuum emission observations, we scanned the sources from −3000" to +3000" with a step of 100". The sources were scanned along both the azimuth and elevation axes. The plots show the variation of observed flux density as a function of angular offset. As in the case of line observations, the data reduction was carried out using the UNIPOPS package. Assuming a gaussian shape for the telescope beam and an unresolved source, we carried out gaussian fit to the profile. The fitted peak give the continuum flux density of the source.

The data obtained from the line and continuum emission observations can be used to find important physical properties of the observed H II regions. The calculations are based on the following assumption: Throughout the HII region,

the temperature is a constant. i.e. the HII region is in thermodynamical equilibrium.

The theoretical and observed r.m.s. noise values are shown in table. The theoretical rms is calculated using the equation,

$$\Delta T_{rms} = T_{sys} / [\beta \tau]^{1/2} K$$

where

β is the channel spacing = (5.920 MHz/4096) = 1.445 kHz

τ is the total integration time.

Spectral Line Analysis

File name	T(system) (K)	Observed rms (Jy)	Calculated rms
17JUN021059C001	**107.6**	**6.206**	**5.2691**
17JUN021224C002	**107.6**	**7.1616**	**6.8053**
15JUN022122C006	**106.5**	**6.6536**	**5.8333**
15JUN022231C008	**106.5**	**6.8005**	**5.8333**
12JUN022310M17	**107.3**	**7.030**	**5.8771**
15JUN022340C013	**106.5**	**6.8771**	**5.8333**

We obtained the following data from the line and continuum observations

Spectral line Obs: Gaussian fit to the spectra

Sources	Peak intensity (Jy)	LSR-velocity (km/s)	ΔV_d (km/s)
M42	16.4	-3.2	29.4
NGC2736	5.0072	0.8686	28.1231
NGC6334	9.7167	-4.8727	22.4674
NGC6357	11.5805	-3.6574	30.9307
M16	5.0406	34.7074	53.6572
M17	29.0988	19.03585	32.0041

Continuum Observations: Gaussian fit to the Source Scans.

Sources	Peak intensity (Jy)	~~Beamwidth~~ SOURCE SIZE	Offset
M42	365.8272	I8' 26.24"	91.15"
NGC2736	172.2765	18' 26.00"	111.59"
NGC6334	163.4857	23' 25.38"	-384.22"
NGC6357	187.7336	24' 25. 16"	142.41"
M16	88.8446	27' 31.58"	82.91"
M17	452.2649	18'37.87"	-368.7"

$2.15 \rightarrow -384.2''$ $90''$

$150''$

$2.16 * 100''$

$= -216''$

5.4 The Electron Temperature, the thermal and turbulence Velocity widths

Sources	Electron temp T_e (K)	Thermal velocity ΔV_{th} (km/s)	Turbulence Velocity ΔV_{tur} (km/s)
M42	9788	21.1668	20.4749
NGC2736	14830	26.0539	10.5879
NGC6334	9691	21.0613	7.8234
NGC6357	7100	18.0266	25.1346
M16	4732	14.7167	51.5996
M17	6649	17.4450	26.8316

The angular size and the distance to the source can be found out from some catalogues. Then we can calculate the solid angle subtended by the source that is given by

$$\Omega = \pi \theta^2$$

where θ is the angular diameter of the source.

The continuum optical depth can be found out using the fomula

$$S_c = 2kT_e(1-\exp[-\tau_C])\Omega/\lambda^2$$

λ is the wavelength of the observed line and S_c is the continuum spectral flux density. Then we can find out the value of continuum emission measure using (Oster 1961)

$$\tau_C = 3.14 \times 10^{-2}[EM_c/T_e^{1.5}\, \nu^2][1.5\ln(T_e/K)-\ln(20.18\nu/GHz)]$$

where,

EM_c = $N_e^2 dl$ pc cm^{-6} is the continuum emission measure. From this we can calculate electron density N_e also, provided that

$$L=D\theta$$

Where D is the distance to the source and θ is the angle subtended by the source. L is the mean diameter of the source.

Sources	Mean d(pc)	OmegaΩ (ster)x10^{-6}	Optical depth τ_C	EM_cx10^6 pc cm^{-6}	Electron density $N_e cm^{-3}$
M42	0.6	1.3362	0.02	3.099	2.273
NGC2736	0.4	0.6358	0.028	7.56	4.347
NGC6334	1.6	0.7073	0.038	5.81	1.906
NGC6357	3.1	395.2	0.001	0.1012	0.326
M16	12.8	4.2537	0.013	0.7718	0.246
M17	5.2	8.0415	0.005	0.4640	0.299

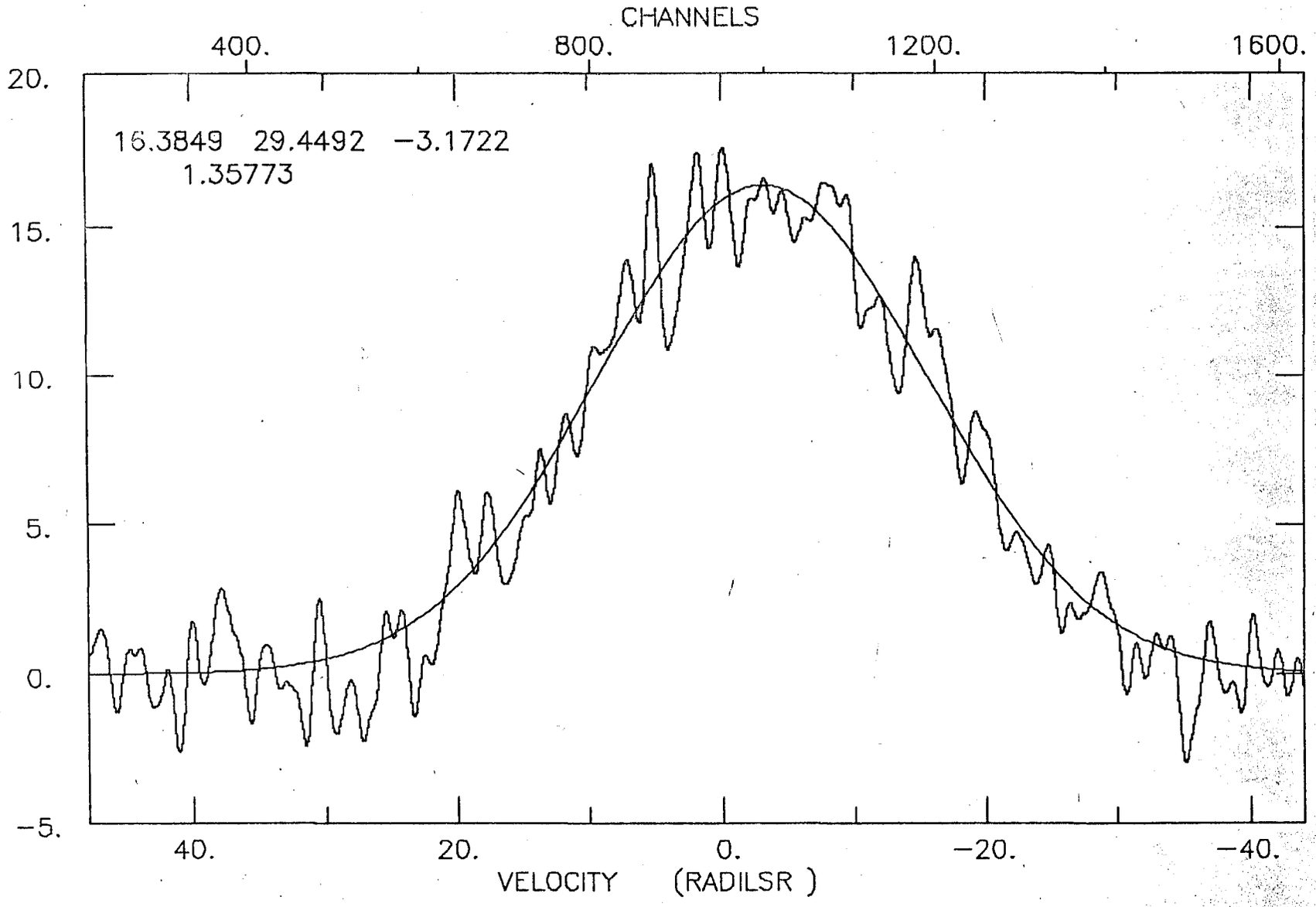

C001 M42 5 SCANS: 33.01- 41.01 INT= 01:09:10 DATE: 18 JUN 2002
APPRADC =05:35:20.9 -05:23:11 CAL= 106.3 TS= 106.
REST= 6676.08000 SKY= 6677.30866 IF=Inf DFREQ= 1.446E-03 DV= 6.50E-02

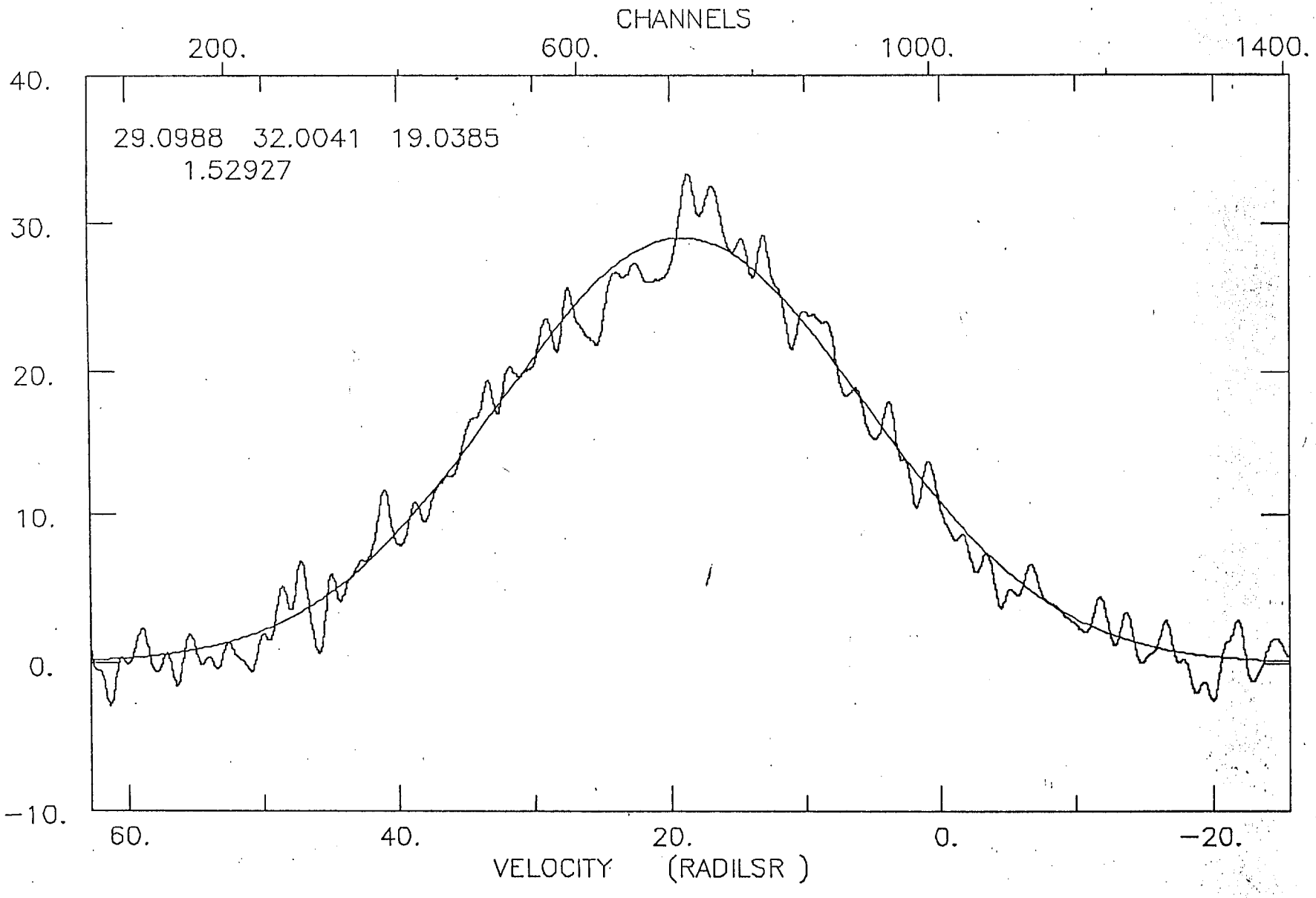

M17 4 SCANS: 123.01− 129.01 INT= 00:55:20 DATE: 13 JUN 2002
APPRADC =18:20:59.9 −16:10:57 CAL= 107.4 TS= 107.
REST= 6676.08000 SKY= 6678.03893 IF=Inf DFREQ= 1.446E−03 DV= 6.50E−02

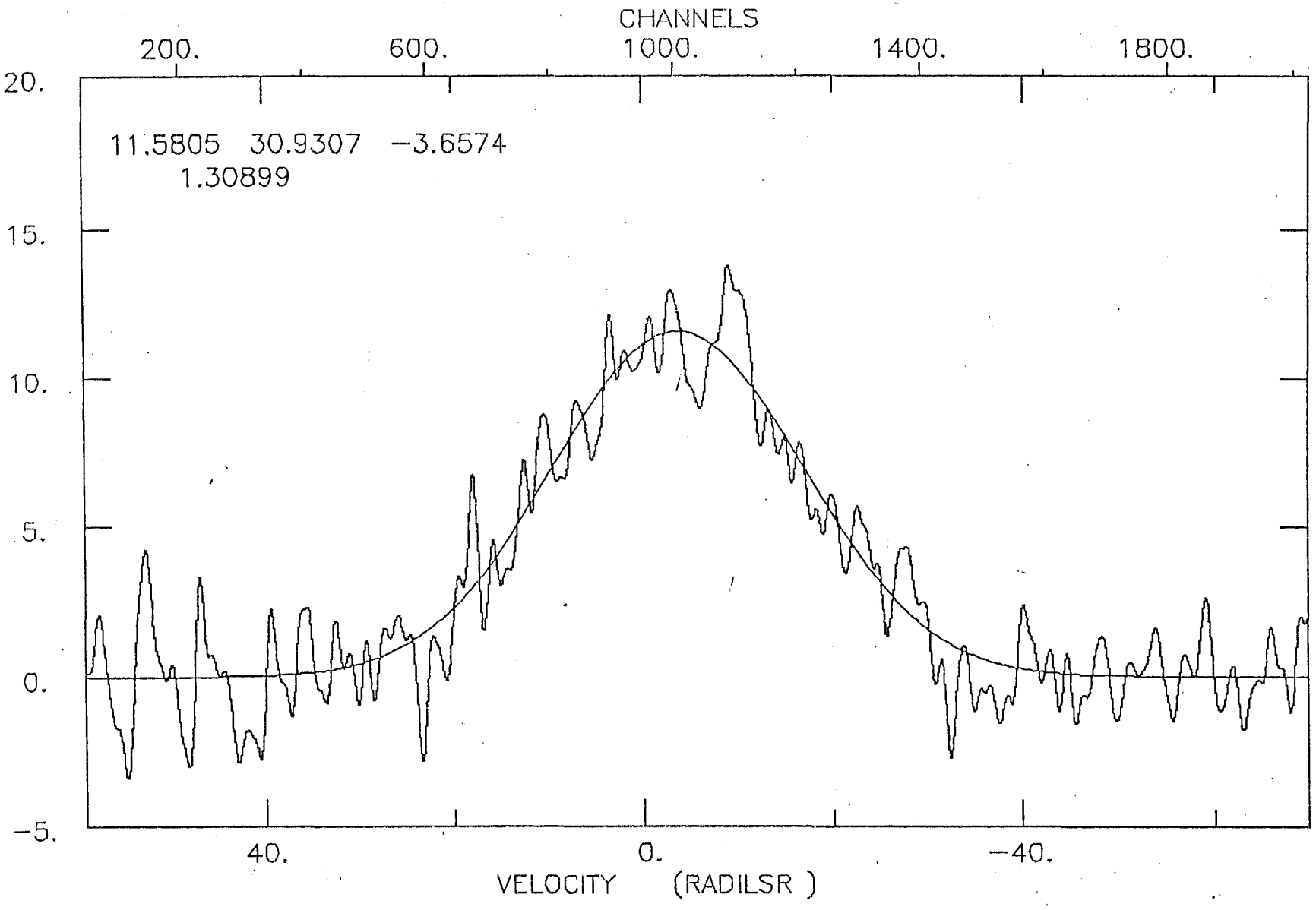

C008 NGC 6357 4 SCANS: 67.01− 73.01 INT= 00:55:20 DATE: 15 JUN 2002
APPRADC =17:25:30.6 −34:22:01 CAL= 106.3 TS= 106.
REST= 6676.08000 SKY= 6677.83261 IF=Inf DFREQ= 1.446E−03 DV= 6.50E−02

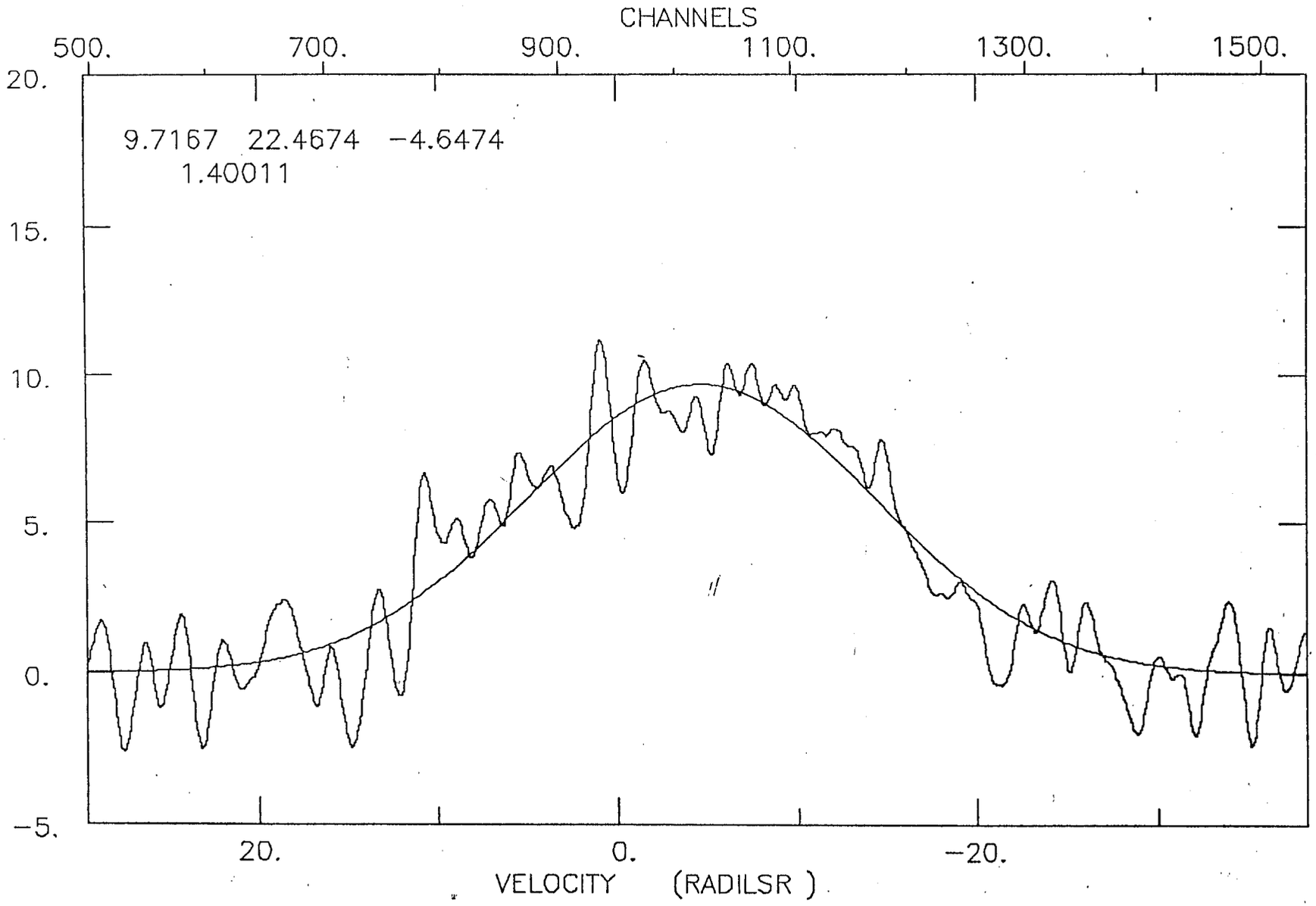

C006 NGC6334 4 SCANS: 229.01− 235.01 INT= 00:55:20 DATE: 15 JUN 2002
APPRADC =17:20:49.2 −35:46:08 CAL= 106.3 TS= 106.
REST= 6676.08000 SKY= 6677.81645 IF=Inf DFREQ= 1.446E−03 DV= 6.50E−02

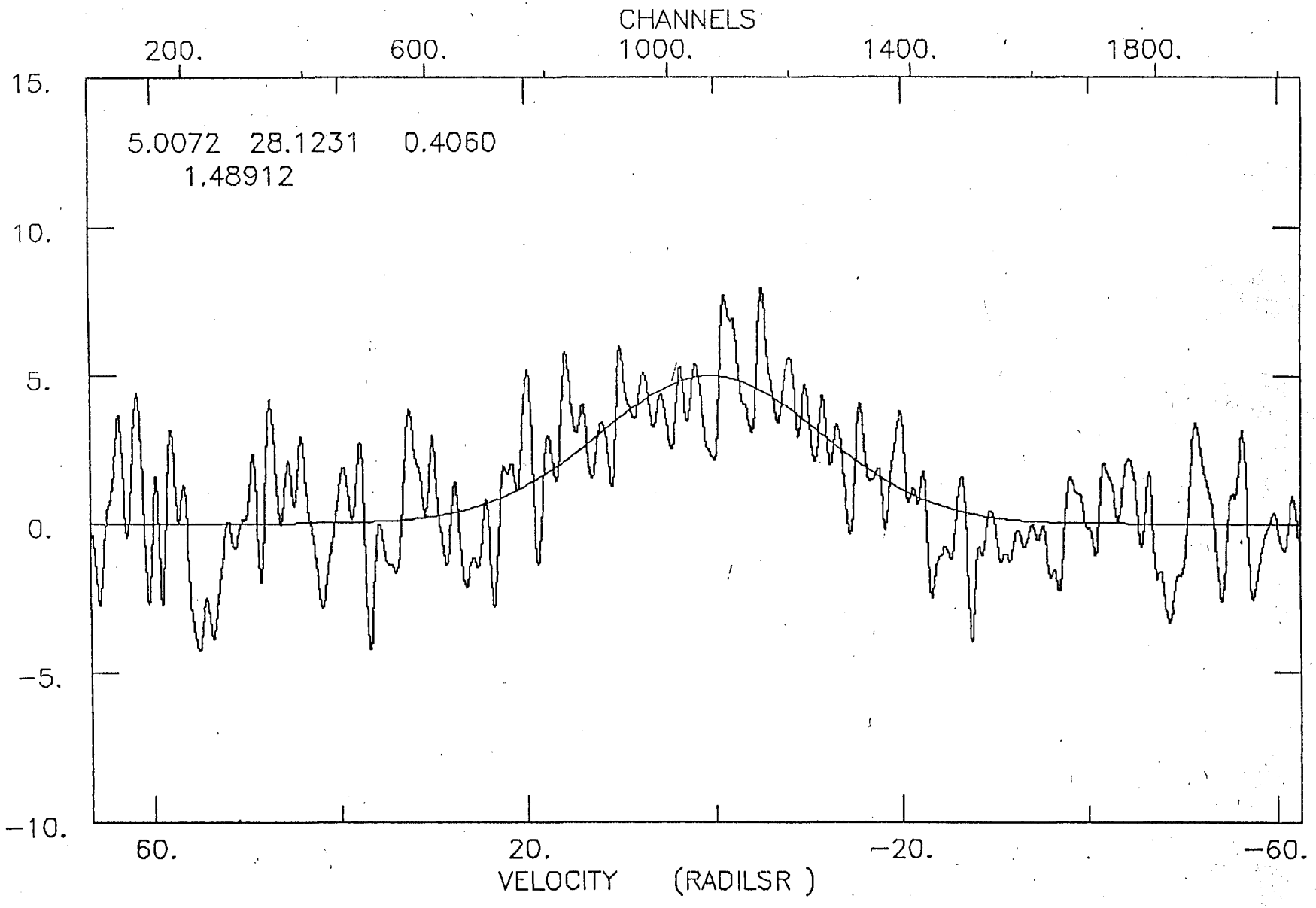

C002 NGC 2736 3 SCANS: 51.01− 57.01 INT= 00:41:30 DATE: 18 JUN 2002
APPRADC =08:59:15.2 −47:35:40 CAL= 106.3 TS= 106.
REST= 6676.08000 SKY= 6676.82264 IF=Inf DFREQ= 1.446E−03 DV= 6.50E−02

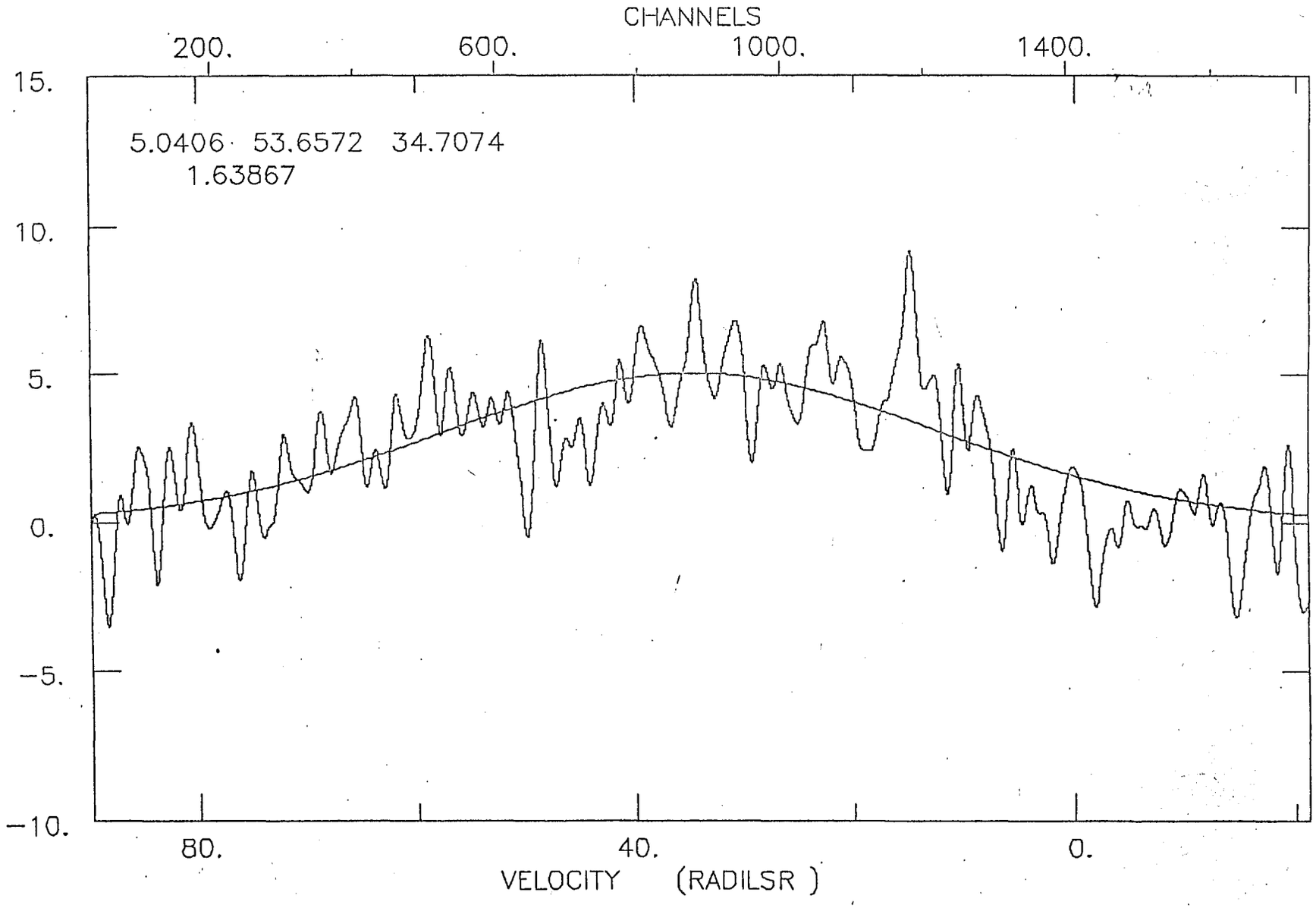

C013 M16 4 SCANS: 131.01− 137.01 INT= 00:55:20 DATE: 15 JUN 2002
APPRADC =18:19: 2.9 −13:45:44 CAL= 106.3 TS= 106.
REST= 6676.08000 SKY= 6677.43825 IF=Inf DFREQ= 1.446E−03 DV= 6.50E−02

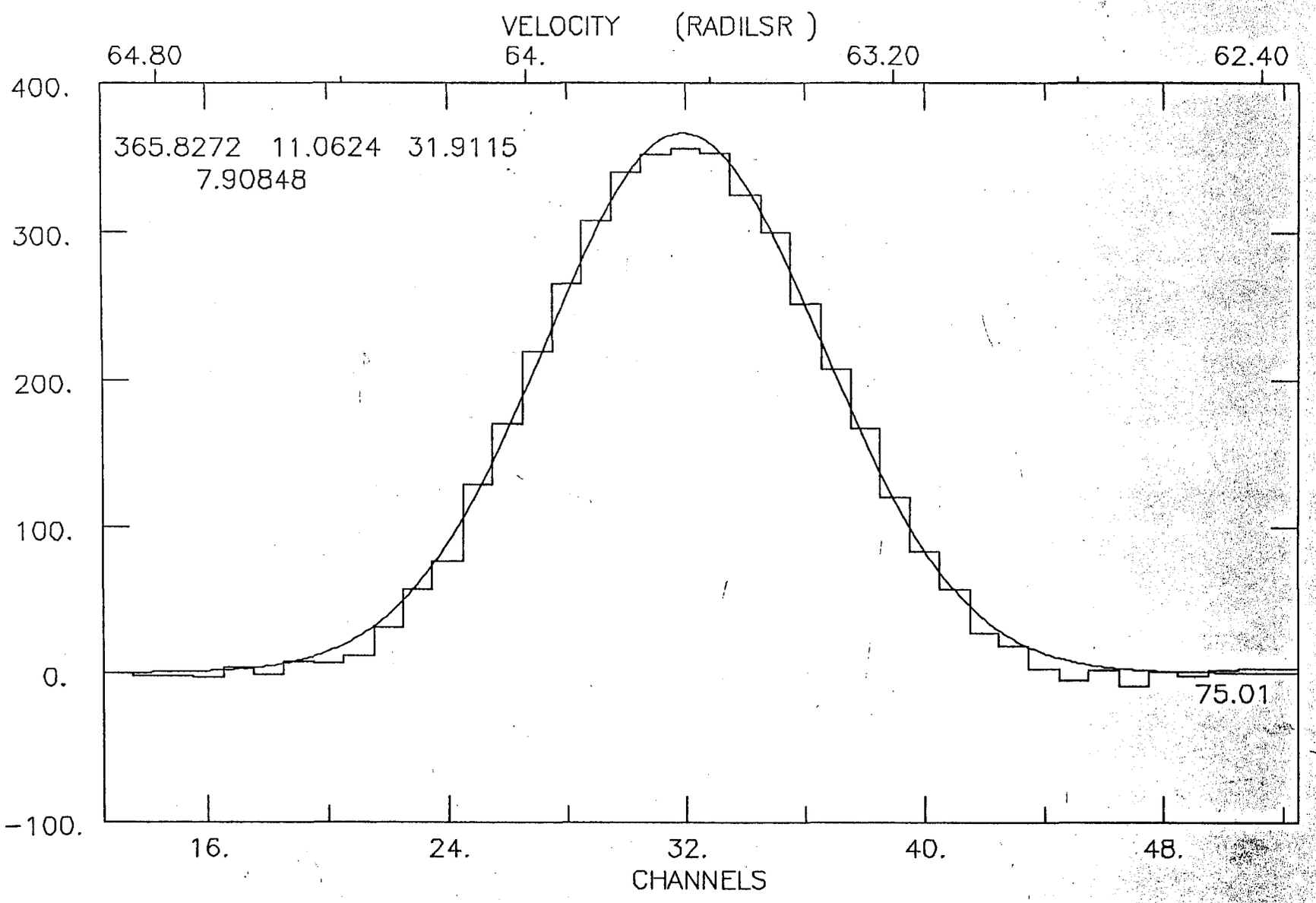
VELOCITY (RADILSR)
64.80
64.
63.20
62.40
400.
300.
200.
100.
0.
-100.
365.8272 11.0624 31.9115
7.90848
75.01
16.
24.
32.
40.
48.
CHANNELS

C001 M42

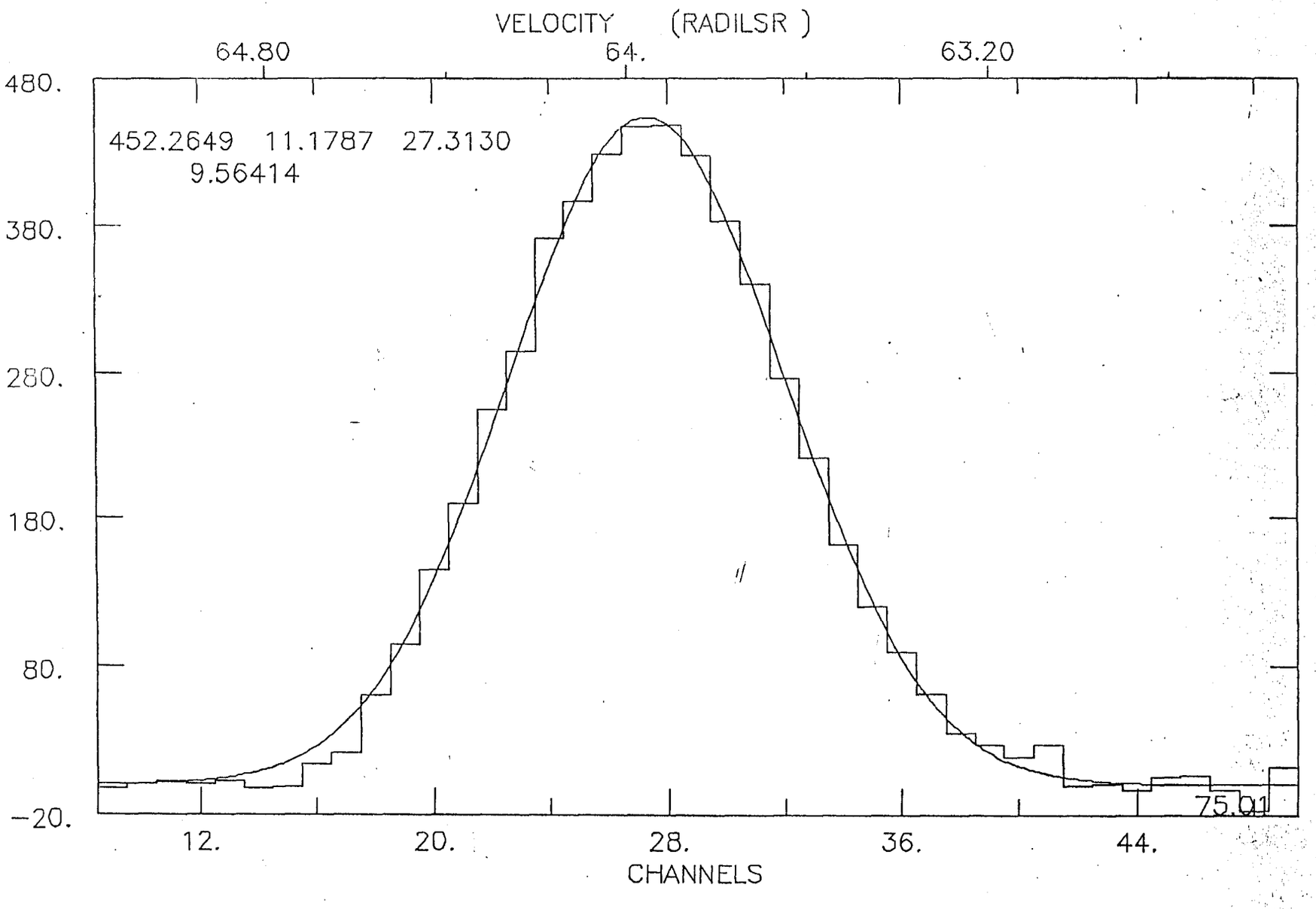
VELOCITY (RADILSR)
64.80
64.
63.20
480.
380.
280.
180.
80.
−20.
452.2649 11.1787 27.3130
9.56414
12.
20.
28.
36.
44.
CHANNELS
75.01

M17

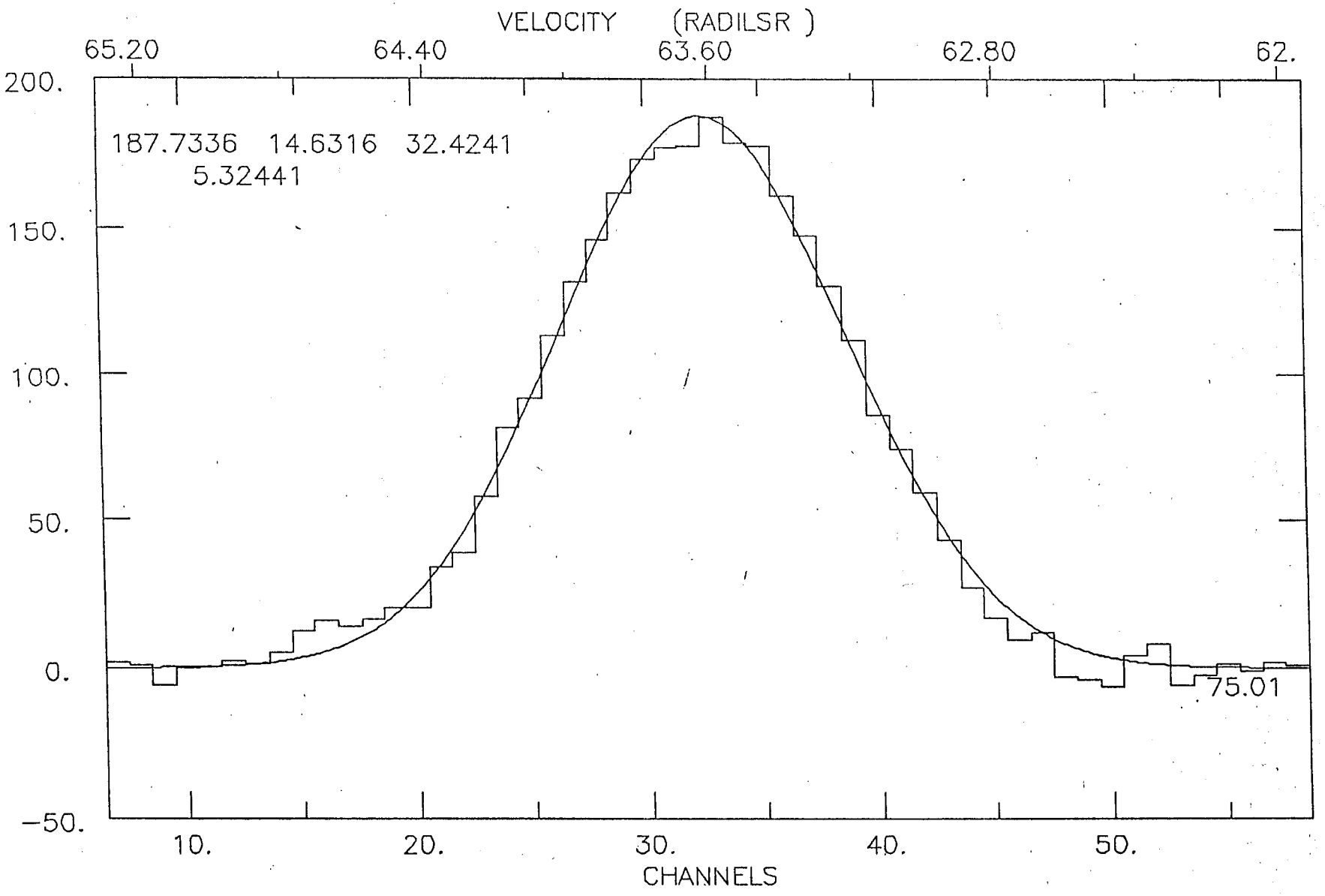

C008 NGC6357

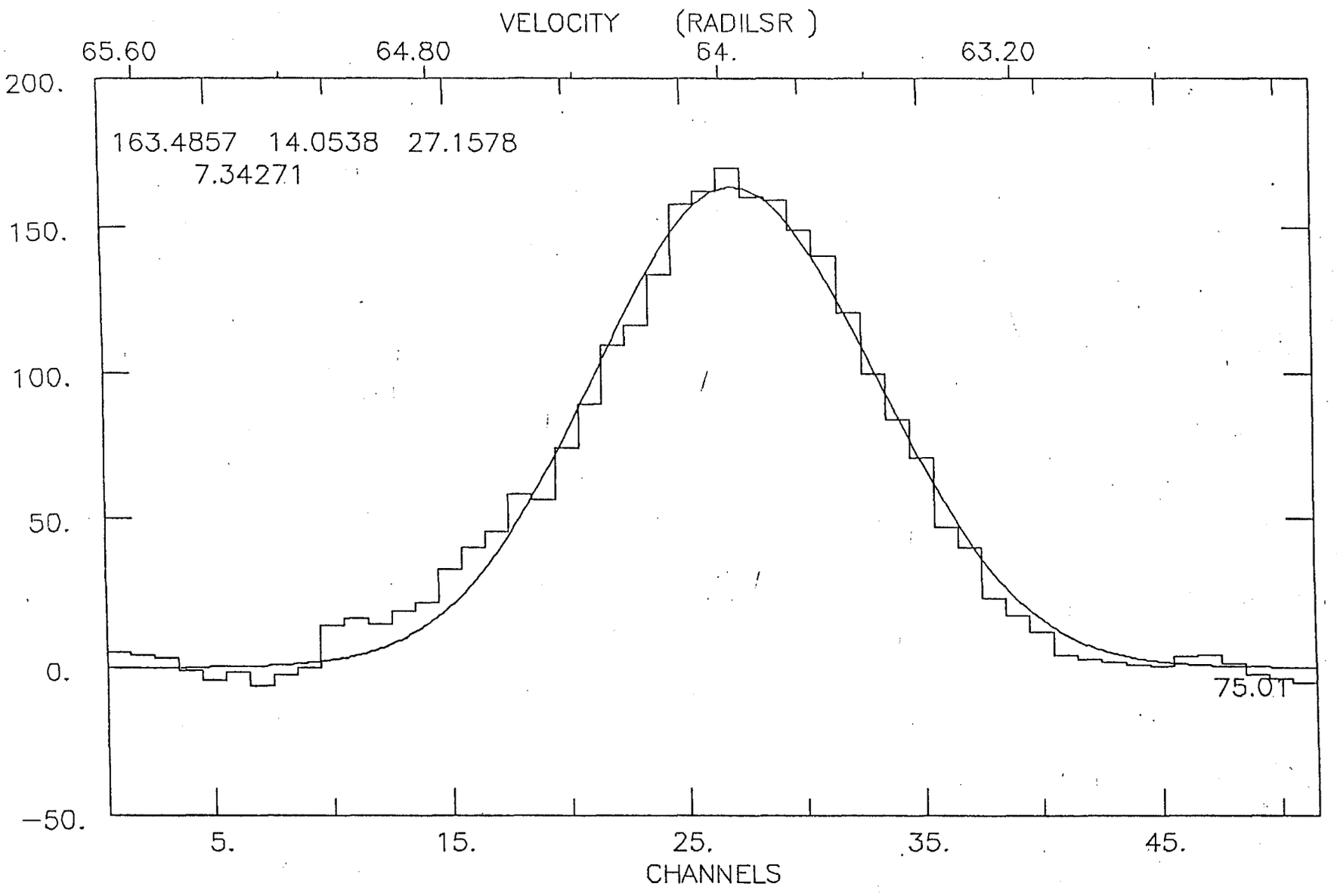

C006 NGC 6334

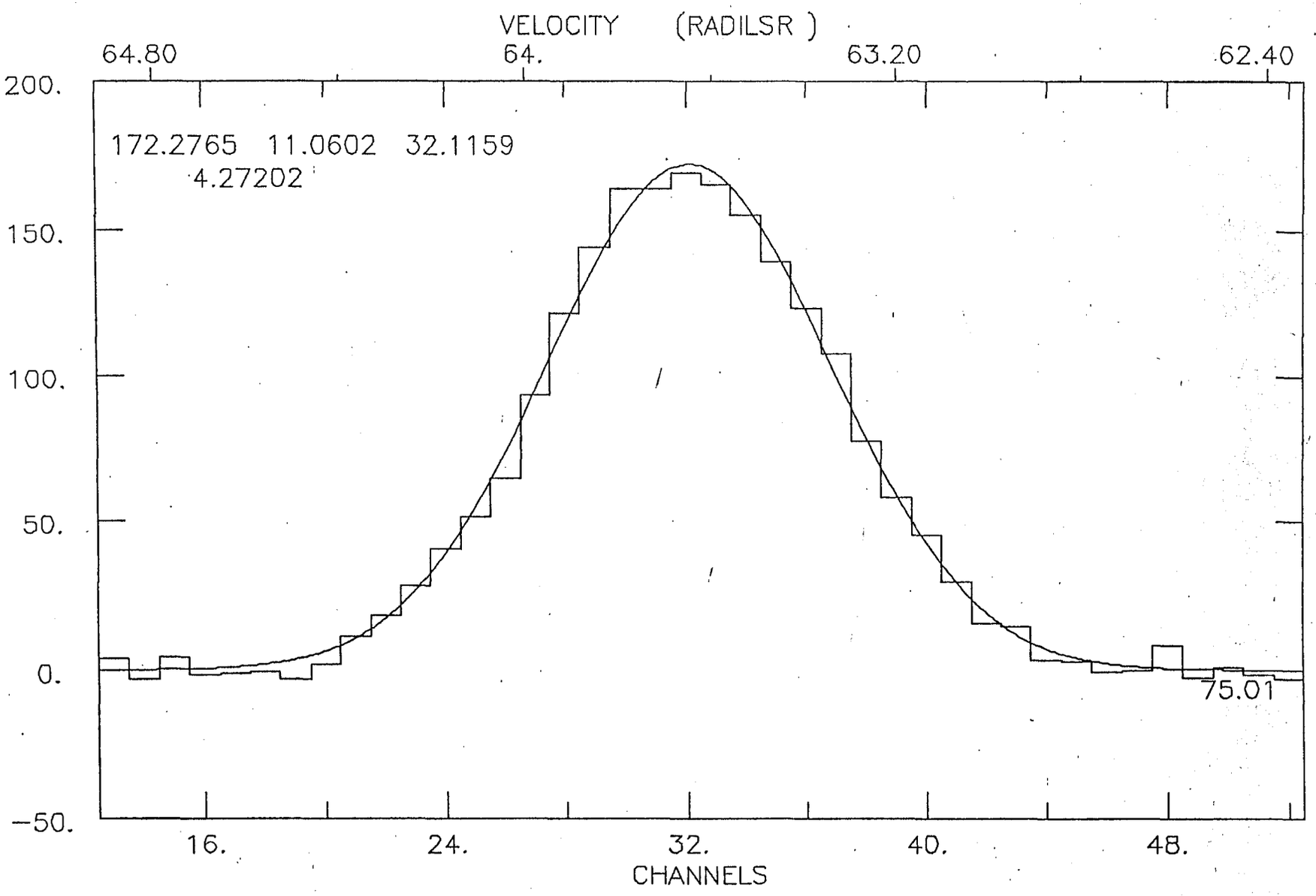

C002 NGC 2736

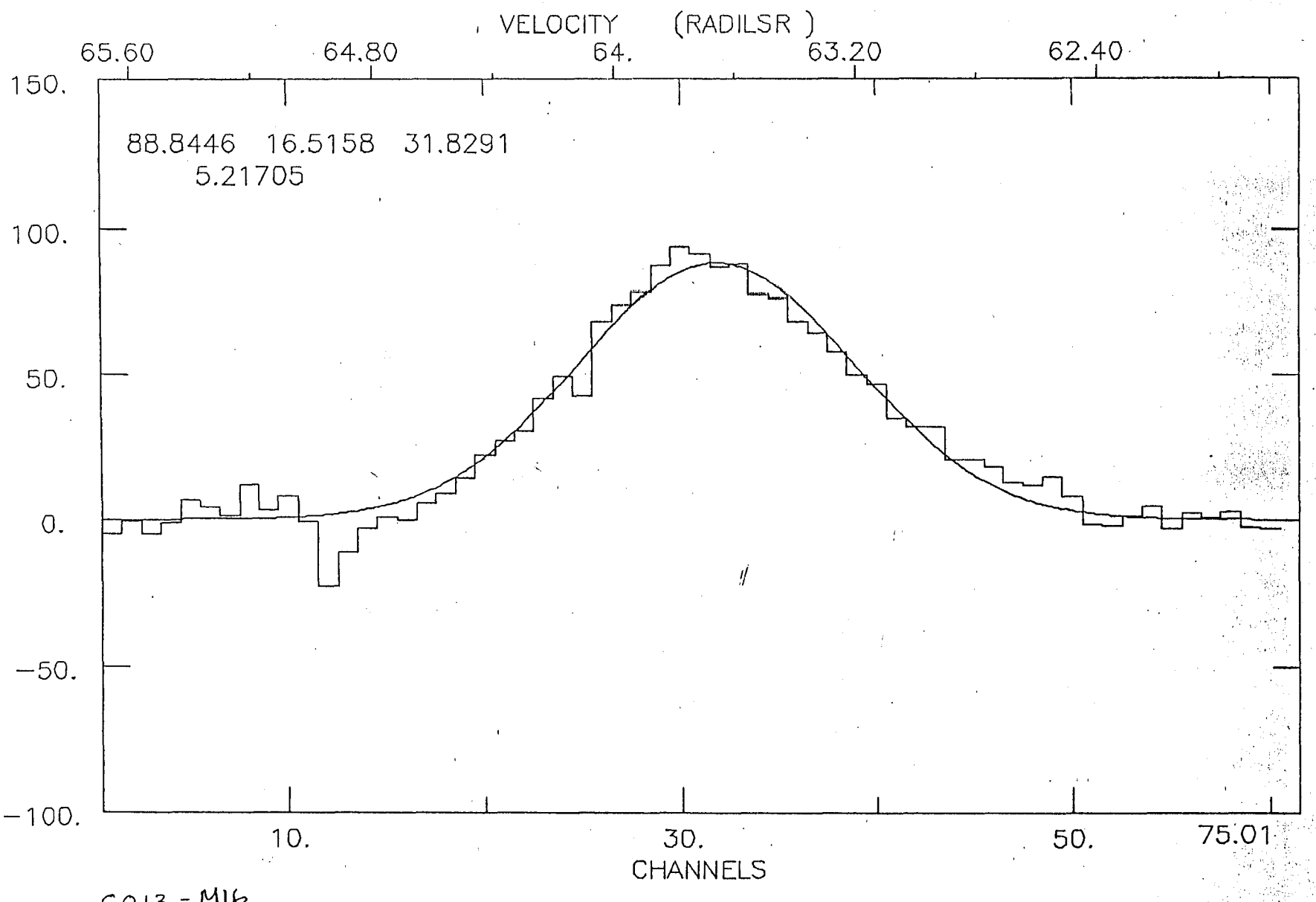
VELOCITY (RADILSR)
65.60
64.80
64.
63.20
62.40
150.
100.
50.
0.
−50.
−100.
88.8446 16.5158 31.8291
5.21705
10.
30.
50.
75.01
CHANNELS

C013 - M16

Appendix A

Single dish Radio Telescopes

A *telescope* is that element of the observing system which fulfils the double role of collecting the electromagentic radiation and forming an image. Radio telescopes are astronomical telescopes used to track celestial objects. They measure radio emissions and are designed to perform certain vital functions. They may be required to measure the intensity of the radiation received from some celestial object and to find out whether this varied with time, to determine the spectrum of the radiation over a certain frequency range or to measure the polarisation of the incoming radiation. Finally, they may be used to produce a detailed map of the brightness distribution over some portion of the sky. The measurements must be made in the presence of interfering emissions coming from other sources in the sky and from the Earth and with additional 'noise' signals generated by the measuring equipment itself.

Imaging in radio astronomy involves antennas of rather large size, requires radio quiet locations and broadband receiving equipment. The reason for using the broadband equipment is that discrete radio objects radiate over a large spectrum, therefore a greater receiver bandwidth increases the amount of energy received from the object.

Filled Aperture Radio Telescopes:

A plane wave that falls on a telescope aperture is brought by reflection or by other means to an output port ('focus') in such a way that the time taken to travel from each point on the incident wavefront to the output port is the same. The most commonly used reflecting surface is the *paraboloid of revolution* or 'parabolic dish'. Parabolic dishes are usually equipped with a single pick-up

point placed at the focus of the paraboloid. The power available at this pick-up point is such that the telescope will measure the flux density from a certain region of the sky centered at the direction towards which the telescope is pointed.In radio terminology this is the region occupied by the *power pattern* or *'beam'* of the telescope.

A parabolic reflector telescope is usually mounted in such a way that it can be steered mechanically to different directions.A map or image of the sky brightness distribution can then be produced by measuring sequentially the flux from a series of directions over the region in question. Many types of refelcting telescope have been used for radio astronomical observations.

Appendix B

RRI 10 .4m Radio telescope:

With the objective of studying the nature and dynamics of clumps of molecular clouds in the galaxy and also the strong maser emission from the dust shells around cool, evolved stars a millimeter wave telescope has been setup at RRI, Bangalore (latitude 13°44.6' N 77°34'59.67" E). The instrument which is steerable has been designed versatile enough to study neutral hydrogen through its 1.42GHz hyperfine transition and to study the rotational and non-rotational motion in the galaxies and the clumpy nature in hydrogen distribution. The telescope which is along the lines of design of CalTech radio telescope has a parabolic reflector of 10.4m diameter with a non corrugated horn for 21cm line observation and a right circular helical feed for observation at 6.7GHz.the parabolic reflector consists of 84 hexagonal panels arranged with a surface accuracy of 250 microns allows for observations with a resolution of 18arcmin at 6.7GHz.

The telescope system can broadly be placed into two sections :

1. The control system.
2. Data acquisition and processing system.

Control system : The telescope has an alt-azimuth mount, with the elevation axis over the azimuth axis. The weight rotating about the elevation axis is 18 tons and about azimuth axis is 3 tons. Tracking a star with this system requires simultaneous movements of both the elevation and azimuth axis for which two pairs of motors are employed. Telescope position information in each axis is obtained from a 21-bit encoder every 100msec. The telescope control system allows us to operate it in three modes manual, local and computer modes. In the

computer mode apart from data acquisition the computer (CPC) also monitors the safety interlock signals.

The control system was built with the following considerations.

1. Stability under varying wind gusts, static and dynamic frictional forces etc.
2. A tracking accuracy of better than 3arc sec at sidereal rates of 15arcsec/sec.
3. Smooth acceleration and deceleration capabilities to avoid stresses on telescope structure and drive system.

Data acquisition and processing system:

This involves all the processing systems right from the conversion of radio waves into signal to obtaining the spectral profile of the radio signal obtained. The typical sensitivity of the telescope is around 3Jy at 6.7GHz (confusion limit). The entire data acquisition and processing can broadly be divided into

1. Reflector and feed.
2. Radio Frequency (RF) section
3. Intermediate Frequency (IF) section
4. Correlation spectrometer.

The 10.4m diameter parabolic reflector receives the radio waves and reflects it to the focal point where the helical feed converts it into a signal. The signal then is passed through the RF section which contains a low noise amplifier and a mixer wher the frequency of the incoming radio signal is down converted to 1.45GHz. This 1.4GHz signal is then fed to the IF section where the signal is sufficiently amplified and the frequency further down converted to 25-35MHz.

In the final section the 25-35MHz band limited signal is quantized and sampled. The digitized signal is then sent to the correlator chips which perform

auto correlation on the signal which later is Fourier transformed (HRSPC) to give the power spectrum of the astronomical signal.

A few important observations which have been carried using the 10.4m telescope are

1. Methanol maser observations at 6.7GHz
2. 21cm neutral hydrogen emission lines at 1420MHz
4. Sio maser lines at 86GHZ